Molecular Pharmacology Fast Forward. Published on June 13, 2006 as doi:10.1124/mol.106.026435
This article has not been copyedited and formatted. The final version may differ from this version.

Involvement of Neuronal Cannabinoid Receptor, CB1, in Regulation of Bone Mass and Bone Remodeling

Joseph Tam*, Orr Ofek*, Ester Fride, Catherine Ledent, Yankel Gabet, Ralph Müller, Andreas Zimmer, Ken Mackie, Raphael Mechoulam, Esther Shohami, Itai Bab

Bone Laboratory, (J.T., O.O., Y.G., I.B.), Department of Medicinal Chemistry and Natural Products (R.M.) and Department of Pharmacology (E.S.), the Hebrew University of Jerusalem, Jerusalem 91120, Israel; Department of Behavioral Sciences (E.F.), College of Judea and Samaria, Ariel 44837, Israel; Institut de Recherche Interdisciplinaire en Biologie Humaine et Moléculaire (I.R.I.B.H.M.) (C.L.), Université Libre de Bruxelles, Campus Erasme, Route de Lennik 808, Brussels, Belgium ; Institute for Biomedical Engineering (R.M.), Swiss Federal Institute of Technology (ETH) and University of Zürich 8044 Zürich, Switzerland; Laboratory of Molecular Neurobiology (A.Z.), Department of Psychiatry, University of Bonn, 53105 Bonn, Germany; Departments of Anesthesiology and Physiology and Biophysics (K.M.), University of Washington, Seattle, WA 98195, U.S.A

Molecular Pharmacology Fast Forward. Published on June 13, 2006 as DOI: 10.1124/mol.106.026435
This article has not been copyedited and formatted. The final version may differ from this version.

Running title: CB1 Cannabinoid Receptor and Bone

Corresponding author: Prof. Itai Bab, Bone Laboratory, the Hebrew University of Jerusalem, P.O.B. 12272, Jerusalem 91120, Israel. Tel.: 972-2-675-8572; Fax: 972-2-675-7623; Email: babi@cc.huji.ac.il

Number of text pages: 19

Number of tables: 1

Number of figures: 5

Number of reference: 23

Number of words in the *Abstract*: 249

Number of words in the *Introduction*: 424

Number of words in the *Results and Discussion*: 1043

Nonstandard abbreviations: $CD1^{CB1-/-}$ mice, CB1-null mice generated on a CD1 background; $C57^{CB1-/-}$ mice, CB1-null mice generated on a C57Bl/6J background; M-CSF, macrophage colony-stimulating factor; TNSALP, tissue non-specific alkaline phosphatase; PTH-Rc1, parathyroid hormone receptor I; TRAP, tartrate-resistant acid phosphatase; BV/TV, trabecular bone volume density; Dia.Dia, diaphyseal shaft diameter; Med.Dia, medullary cavity diameter.

Molecular Pharmacology Fast Forward. Published on June 13, 2006 as DOI: 10.1124/mol.106.026435
This article has not been copyedited and formatted. The final version may differ from this version.

Abstract

Recently, the CB1 cannabinoid receptor was implicated in the regulation of bone remodelling and bone mass. A high bone mass (HBM) phenotype was reported in CB1-null mice generated on a CD1 background ($CD1^{CB1-/-}$ mice). By contrast, our preliminary studies in *cb1*$^{-/-}$ mice, backcrossed to C57Bl/6J mice ($C57^{CB1-/-}$ mice), revealed low bone mass (LBM). We therefore analyzed CB1 expression in bone and compared the skeletons of sexually mature $C57^{CB1-/-}$ and $CD1^{CB1-/-}$ mice in the same experimental setting. CB1 mRNA is weakly expressed in osteoclasts and immunoreactive CB1 is present in sympathetic neurons, close to osteoblasts. In addition to their LBM, male and female $C57^{CB1-/-}$ mice exhibit decreased bone formation rate and increased osteoclast number. The skeletal phenotype of the $CD1^{CB1-/-}$ mice shows a gender disparity. Females have normal trabecular bone with a slight cortical expansion, whereas male $CD1^{CB1-/-}$ animals display a HBM phenotype. Surprisingly, bone formation and resorption are within normal limits. These findings, at least the consistent set of data obtained in the $C57^{CB1-/-}$ line, suggest an important role for CB1 signalling in the regulation of bone remodelling and bone mass. Because sympathetic CB1 signalling inhibits norepinephrine (NE) release in peripheral tissues, part of the endocannabinoid activity in bone may be attributed to the regulation of NE release from sympathetic nerve fibers. Several phenotypic discrepancies have been reported between $C57^{CB1-/-}$ and $CD1^{CB1-/-}$ mice, which could result from genetic differences between the background strains. Unraveling these differences can provide useful information on the physiologic functional milieu of CB1 in bone.

Molecular Pharmacology Fast Forward. Published on June 13, 2006 as DOI: 10.1124/mol.106.026435
This article has not been copyedited and formatted. The final version may differ from this version.

The endogenous cannabinoids bind to and activate the CB1 and CB2 cannabinoid receptors. Both are seven-transmembrane domain receptors which share 44% identity. They are coupled to the Gi/o subclass of G-proteins and inhibit stimulated adenylyl cyclase activity (Rhee et al., 1997). CB1 is present in the brain and in peripheral neurons and accounts for most of the central nervous system actions of cannabinoid drugs and endocannabinoids (Herkenham et al., 1990; Zimmer et al., 1999). CB2 is found mainly in the immune system (Munro et al., 1993).

In vertebrates, bone mass and shape are determined by continuous remodeling consisting of the concerted and balanced action of osteoclasts, the bone resorbing cells, and osteoblasts, the bone forming cells. Osteoporosis, the most prevalent degenerative disease in developed countries, results from impaired remodeling balance, which leads to bone loss and increased fracture risk. It has been recently reported that bone remodeling is subject to central control through pathways that involve signaling by the hypothalamic receptors for leptin and neuropeptide Y (Ducy et al., 2000; Baldock et al., 2002), which are also associated with the regulation of endocannabinoid brain levels (Di Marzo et al., 2001). Along these lines we have recently reported that (i) the peripheral CB2 cannabinoid receptor is normally expressed in osteoblasts, osteoclasts and in their precursors; (ii) mice deficient for CB2 have a low bone mass (LBM) phenotype; (iii) specific activation of CB2 attenuates ovariectomy-induced bone loss by restraining osteoclastogenesis and stimulating bone formation (Ofek et al., 2006).

Two mutant mouse lines with deficiency in the CB1 gene have been generated. In one line, backcrossed to C57Bl/6J mice ($C57^{CB1-/-}$), almost the entire protein-encoding sequence was removed (Zimmer et al., 1999). In the other line, backcrossed to CD1 mice ($CD1^{CB1-/-}$), the N-terminal 233 codons of *cb1* were ablated (Ledent et al., 1999). Although both lines demonstrate a null mutation missing all the CB1 responsiveness to cannabinoid ligands, they display significant phenotypic discrepancies (Lutz, 2002; Hoffman et al., 2005). Regarding

Molecular Pharmacology Fast Forward. Published on June 13, 2006 as DOI: 10.1124/mol.106.026435
This article has not been copyedited and formatted. The final version may differ from this version.

the skeleton, it has been recently published that $CD1^{CB1-/-}$ mice have a high bone mass (HBM) phenotype, suggesting that activation of CB1 down regulates bone mass (Idris et al., 2005). By contrast, our preliminary studies in $C57^{CB1-/-}$ mice pointed to a LBM phenotype occurring in the absence of functional CB1 receptors. These studies used different methods to characterize the skeletal phenotype. Hence, in an attempt to solve this critical discrepancy, we analyzed the expression and distribution of CB1 in bone and compared the skeletons of the $C57^{CB1-/-}$ and $CD1^{CB1-/-}$ mouse lines using identical methods, equipment and expertise.

Materials and Methods

Animals. All animals in the study were 9 to 12-week-old mice. $C57^{CB1-/-}$ mice were generated as reported previously (Zimmer et al., 1999). We have crossed heterozygous animals of this line for at least 10 generations to WT C57BL/6J mice. Heterozygous animals from the last generation were then intercrossed to obtain congenic C57BL/6J mice that are homozygous for the respective mutation. $CD1^{CB1-/-}$ mice were generated by homologous recombination as described previously (Ledent et al., 1999). Heterozygous mice were bred for 17 generations on a CD1 background before generating the WT and *cb1* null littermates used in this study. To study bone formation, newly formed bone was vitally labelled in mice intended for micro-computed tomographic (μCT)-histomorphometric analysis by the fluorochrome calcein (Sigma), injected intraperitoneally (15 mg/Kg) four days and one day prior to sacrifice. The use of animals was approved by the Institutional Animal Care Committee of the Hebrew University of Jerusalem.

Immunohistochemistry. Mice were killed by transcardial perfusion of phosphate buffered saline followed by 4% parafomaldehyde. The femora were dissected and further fixed with parafomaldehyde for 2 h at 4°C. The specimens were decalcified in 0.5 M EDTA, pH 7.4 and embedded in paraffin. For immunohistochemical analysis, 5 μm serial frontal sections were reacted with anti-tyrosine hydroxylase (TH) (Chemicon, Temecula, CA) or anti-CB1 antibodies (Nyíri et al., 2005). Further processing was carried out using the *SuperPicture*™ Polymer detection Kit (Zymed Laboratories, San Francisco, CA; cat no. 87-9263) according to the manufacturer instructions.

Cell cultures and mRNA analysis. Primary bone marrow stromal cell cultures from WT adult femoral and tibial diaphyseal bone marrow were established as previously described. For testing CB1 expression, the cells were grown in osteogenic medium (Ofek et al, 2006). Bone marrow derived osteoclastogenic cultures were established from ficoll-

Molecular Pharmacology Fast Forward. Published on June 13, 2006 as DOI: 10.1124/mol.106.026435
This article has not been copyedited and formatted. The final version may differ from this version.

separated monocytic precursors and grown for 5-6 days in medium containing macrophage colony-stimulating factor (M-CSF) and RANK ligand (RANKL) (R&D Systems) (Ofek et al., 2006). Total RNA was extracted from the cells, purified and reverse transcribed using routine procedures. The following primers were used for PCR: CB1, sense: 5'-TGGTGTATGATGTCTTTGGG-3', antisense: 5'-ATGCTGGCTGTGTTATTGGC-3'; tissue non-specific alkaline phosphatase (TNSALP), sense: 5'-GACA-CAAGCATTCCCACTAT-3', antisense: 5'-ATCAG-CAGTAACCACAGTCA-3'; parathyroid hormone receptor I (PTH-Rc1), sense: 5'-CAAGAAGTGGATCATCCAGGT-3', antisense: 5'-GCTGCTACTCCCACTTCGTGCTTT-3'; β-actin, sense, 5'-GAGACCTTCAACACCCCAGCC-3'; antisense, 5'- GGCCATCTCTTGCTCGAAGTC-3'.

Microcomputed Tomographic (μCT) Analysis. Whole femora were examined by a μCT system (μCT 40, SCANCO Medical, Bassersdorf, Switzerland) as reported recently (Bajayo et al., 2005; Ofek et al., 2006). Scans were performed at a resolution of 20 μm in all three spatial dimensions. Morphometric parameters were determined as reported previously (Kram et al., 2006). Trabecular and cortical bone parameters were measured in metaphyseal and mid-diaphyseal segments, respectively.

Histomorphometry. After μCT image acquisition, the specimens were embedded undecalcified in Technovit 9100 (Heraeus). Longitudinal sections through the midfrontal plane were left unstained for dynamic histomorphometry, based on the vital calcein double labeling. To identify osteoclasts, consecutive sections were stained for tartrate-resistant acid phosphatase (TRAP). Parameters were determined according to a standardized nomenclature (Parfitt et al., 1987).

Statistical analysis. Differences between *cb1*$^{-/-}$ and WT mice were analyzed by the Student's t-test.

Molecular Pharmacology Fast Forward. Published on June 13, 2006 as DOI: 10.1124/mol.106.026435
This article has not been copyedited and formatted. The final version may differ from this version.

Results and Discussion

Expression of CB1 in bone. mRNA analyses were carried out in cells derived from WT C57Bl/6J mice. Unlike the expression of CB2, which is absent in undifferentiated bone marrow stromal cells, but increases progressively when these cells undergo osteoblastic differentiation (Ofek et al., 2006), we were unable to identify CB1 mRNA transcripts in either undifferentiated or differentiated stromal cells, even after 40 PCR cycles (Fig. 1A). Monocytic osteoclast precursors from these mice also did not show CB1 expression. Yet, a weak signal was present when these cells underwent osteoclastogenesis with M-CSF and RANKL (Fig. 1B).

Bone, especially trabecular, is densely innervated by sympathetic fibers (Serre et al, 1999; Mach et al., 2002). These fibers release norepinephrine (NE), thus potently mediating central signals that restrain bone formation and stimulate bone resorption (Elefteriou et al., 2005). Because CB1 is expressed in such nerve fibers elsewhere (Schlicker and Kathmann, 2001), we further explored its presence in bone sympathetic nerve fibers. Indeed, immunohistochemical analysis using the sympathetic marker TH (Bjurholm et al., 1988) confirmed the occurrence of a network of TH-positive fibers in the inter-trabecular spaces of cancellous bone in both C57Bl/6J and CD1 mice (Figs. 1C, 1G). The fibers were close to the bone trabeculae with terminal nerve processes penetrating the osteoblast palisades, thus being in intimate proximity to these cells (Figs. 1D, 1G). Consecutive histological sections show CB1 immunoreactivity of the same nerve fibers (Figs. 1E, 1F, 1H), indicating the presence of CB1 receptors in sympathetic fibers that innervate the trabecular bone. This CB1 immunoreactivity was missing in the CB1-null mice (data not shown).

Skeletal phenotype of CB1-null mice. Our results demonstrate that the background WT strains, in which the $C57^{CB1-/-}$ and $CD1^{CB1-/-}$ mouse lines had been established, display

Molecular Pharmacology Fast Forward. Published on June 13, 2006 as DOI: 10.1124/mol.106.026435
This article has not been copyedited and formatted. The final version may differ from this version.

vast differences in both trabecular and cortical bone mass. More importantly, *cb1* inactivation in these lines resulted in opposing skeletal effects (Figs. 2-4).

Compared to their WT controls, both male and female $C57^{CB1-/-}$ mice exhibited low bone mass (LBM) phenotype characterized by a lower density of their trabecular network. The trabecular bone volume density (BV/TV) in female and male null mice was lower by 20% and 15% than that of WT C57Bl/6J controls, respectively (Fig. 2). Apparently, the lower BV/TV in the $C57^{CB1-/-}$ mice resulted from decreases in the trabecular number (Fig. 3A) without changes in the trabecular thickness (Tb.Th) (Fig. 3B). The trabecular connectivity density, a parameter measuring the structural integrity of the trabecular network (Stampa et al., 2002), was also decreased in these animals (Fig. 3C) but did not reach statistical difference. Also, both the diaphyseal shaft diameter (Dia.Dia) and medullary cavity diameter (Med.Dia) were narrower in the $C57^{CB1-/-}$ mice (Fig. 4A & 4B), with unchanged cortical thickness (Fig. 4C).

By contrast, the $CD1^{CB1-/-}$ skeletal phenotype showed a marked gender bias. The trabecular bone, the main skeletal compartment affected in osteoporosis, appears normal in female $CD1^{CB1-/-}$ mice (Figs. 2, 3D-3F). Male $CD1^{CB1-/-}$ mice had a pronounced HBM phenotype demonstrating 27.5% increase in trabecular BV/TV (Fig. 2) accompanied by increased Tb.Th (Fig. 3E) and slightly decreased connectivity density (Fig. 3F). The female $CD1^{CB1-/-}$ diaphysis was mildly abnormal, exhibiting cortical expansion portrayed as increases in both Dia.Dia and Med.Dia (Figs. 4D, 4E). The male $CD1^{CB1-/-}$ diaphysis appeared normal (Fig. 4D-4F).

To gain further insight into the processes leading to the LBM phenotype in $C57^{CB1-/-}$ mice, we analyzed their bone remodelling. Consistent with the results of the structural μCT parameters, the histomorphometric analysis demonstrated that the LBM in these mice is associated with unbalanced bone remodelling. The bone formation rate (BFR) was markedly

Molecular Pharmacology Fast Forward. Published on June 13, 2006 as DOI: 10.1124/mol.106.026435
This article has not been copyedited and formatted. The final version may differ from this version.

decreased in both females and males (Fig. 5A), mainly due to a decrease in mineral appositional rate, a surrogate of osteoblast activity (Fig. 5B), inasmuch as the mineralizing perimeter, a surrogate of osteoblast number, remains unchanged (Fig. 5C). The osteoclast number was increased, significantly in females and insignificantly in males (Fig. 5D). Unexpectedly, we could not find any significant differences in bone remodelling parameters between the $CD1^{CB1-/-}$ mice and their WT controls, even not in males (Table 1). Jointly these results suggest that in the C57Bl/6J mice, CB1 signalling positively regulates trabecular bone mass and radial diaphyseal growth by up regulating bone formation and down regulating bone resorption. The absence of significant changes in bone remodelling parameters of the male $CD1^{CB1-/-}$ mice suggests that CB1 in these animals is associated only with the accrual of peak bone mass, which occurs at a younger age than that studied here. Apparently, the LBM phenotype is exhibited in the $C57^{CB1-/-}$ mice consequent to a decrease in bone formation and increase in bone resorption attributable to the absence of sympathetic CB1, which normally inhibits NE release (Ishac et al., 1996).

Although either genetic modification lead to a null mutation missing all CB1 responsiveness to its ligands, the occurrence of phenotypic differences is not entirely surprising, inasmuch as these mouse lines exhibit other substantial discrepancies ranging from nociceptive perception to locomotor activity, life expectancy and embryo implantation (Lutz, 2002). Furthermore, at least to some extent, skeletal dissimilarity between the $C57^{CB1-/-}$ and $CD1^{CB1-/-}$ mice could be expected from the differences in bone mass and structure observed between the WT CD1 and C57Bl/6J background strains. More surprising is the gender bias portrayed by the $CD1^{CB1-/-}$ mice and the absence of changes in bone remodeling in male animals that could explain their HBM. Although a HBM phenotype, unaccompanied by changes in bone remodeling, was reported previously (Idris et al., 2005), it is unclear to us whether it was assigned to males, females or both.

Molecular Pharmacology Fast Forward. Published on June 13, 2006 as DOI: 10.1124/mol.106.026435
This article has not been copyedited and formatted. The final version may differ from this version.

In spite of the differences between the two mouse lines, the present findings, especially the consistency in $C57^{CB1-/-}$ mice presented by (i) CB1 expression in bone; (ii) LBM; and (iii) changes in skeletal turnover parameters, suggest a role for sympathetic CB1 in the control of bone remodeling and bone mass. In fact, unraveling the genetic differences between the C57Bl/6J and CD1 strains, as well as the genetic basis for the gender discrimination within the $CD1^{CB1-/-}$ mouse line, can provide useful information on the physiologic functional milieu of CB1 in bone. Until an explanation for the skeletal (and possibly other) differences between the $C57^{CB1-/-}$ and $CD1^{CB1-/-}$ mice is found, it is our approach that only experimental trends shared by both mouse lines should be considered.

Molecular Pharmacology Fast Forward. Published on June 13, 2006 as DOI: 10.1124/mol.106.026435
This article has not been copyedited and formatted. The final version may differ from this version.

Acknowledgements

The authors thank Olga Lahat, Malka Attar, Meirav Fogel and Dr. Ravit Birenboim for their expert assistance. ES and RM are affiliated with the David R. Bloom Centre for Pharmacy, The Hebrew University School of Pharmacy, Jerusalem, Israel.

References

Bajayo A, Goshen I, Feldman S, Csernus V, Iverfeldt K, Shohami E, Yirmiya R and Bab I (2005) Central IL-1 receptor signaling regulates bone growth and mass. *Proc Natl Acad Sci U S A* **102**:12956-12961.

Baldock PA, Sainsbury A, Couzens M, Enriquez RF, Thomas GP, Gardiner EM and Herzog H (2002) Hypothalamic Y2 receptors regulate bone formation. *J Clin Invest* **109**:915–921**.**

Bjurholm A, Kreicbergs A, Terenius L, Goldstein M and Schultzberg M (1988) Neuropeptide Y-, tyrosine hydroxylase- and vasoactive intestinal polypeptide-immunoreactive nerves in bone and surrounding tissues. *J Auton Nerv Syst* **25**:119-125.

Di Marzo V, Goparaju SK, Wang L, Liu J, Batkai S, Jarai Z, Fezza F, Miura GI, Palmiter RD, Sugiura T and Kunos G (2001) Leptin-regulated endocannabinoids are involved in maintaining food intake. *Nature* **410**:822–825.

Ducy P, Amling M, Takeda S, Priemel M, Schilling AF, Beil FT, Shen J, Vinson C, Rueger JM and Karsenty G (2000) Leptin inhibits bone formation through a hypothalamic relay: a central control of bone mass. *Cell* **100**:197–207**.**

Elefteriou F, Ahn JD, Takeda S, Starbuck M, Yang X, Liu X, Kondo H, Richards WG, Bannon TW, Noda M, Clement K, Vaisse C and Karsenty G (2005) Leptin regulation of bone resorption by the sympathetic nervous system and CART. *Nature* **434**:514-520**.**

Herkenham M, Lynn AB, Little MD, Johnson MR, Melvin LS, de Costa BR and Rice KC (1990) Cannabinoid receptor localization in brain. *Proc Natl Acad Sci USA* **87**:1932–1936.

Hoffman AF, Macgill AM, Smith D, Oz M and Lupica CR (2005) Species and strain differences in the expression of a novel glutamate-modulating cannabinoid receptor in the rodent hippocampus. *Eur J Neurosci* **22**:2387-2391.

Idris AI, van 't Hof RJ, Greig IR, Ridge SA, Baker D, Ross RA and Ralston SH (2005) Regulation of bone mass, bone loss and osteoclast activity by cannabinoid receptors. *Nat Med* **11**:774-779.

Ishac EJ, Jiang L, Lake KD, Varga K, Abood ME and Kunos G (1996) Inhibition of exocytotic noradrenaline release by presynaptic cannabinoid CB1 receptors on peripheral sympathetic nerves. *Br J Pharmacol* **118**:2023-2028.

Ledent C, Valverde O, Cossu G, Petitet F, Aubert JF, Beslot F, Bohme GA, Imperato A, Pedrazzini T, Roques BP, Vassart G, Fratta W and Parmentier M (1999) Unresponsiveness to cannabinoids and reduced addictive effects of opiates in CB1 receptor knockout mice. *Science* **283**:401-404.

Kram V, Zcharia E, Yacoby-Zeevi O, Metzger S, Chajek-Shaul T, Gabet Y, Muller R, Vlodavsky I and Bab I (2006) Heparanase is expressed in osteoblastic cells and stimulates bone formation and bone mass. *J Cell Physiol* **207**:784-792.

Lutz B (2002) Molecular biology of cannabinoid receptors. *Prostaglandins Leukot Essent Fatty Acids* **66**:123-142.

Mach DB, Rogers SD, Sabino MC, Luger NM, Schwei MJ, Pomonis JD, Keyser CP, Clohisy DR, Adams DJ, O'Leary P and Mantyh PW (2002) Origins of skeletal pain: sensory and sympathetic innervation of the mouse femur. *Neuroscience* **113**:155-166.

Munro S, Thomas KL and Abu-Shaar M (1993) Molecular characterization of a peripheral receptor for cannabinoids. *Nature* **365:**61–65.

Nyíri G, Cserep C, Szabadits E, Mackie K and Freund TF (2005) CB1 cannabinoid receptors are enriched in the perisynaptic annulus and on preterminal segments of hippocampal GABAergic axons. *Neuroscience* **136**:811-822

Ofek O, Karsak M, Leclerc N, Fogel M, Frenkel B, Wright K, Tam J, Attar-Namdar M, Kram V, Shohami E, Mechoulam R, Zimmer A and Bab I (2006) Peripheral cannabinoid receptor, CB2, regulates bone mass. *Proc Natl Acad Sci U S A* **103**:696-701.

Parfitt AM, Drezner MK, Glorieux FH, Kanis JA, Malluche H, Meunier PJ, Ott SM and Recker RR (1987) Bone histomorphometry: standardization of nomenclature, symbols, and units. Report of the ASBMR Histomorphometry Nomenclature Committee. *J Bone Miner Res* **2**:595–610.

Rhee MH, Vogel Z, Barg J, Bayewitch M, Levy R, Hanus L, Breuer A and Mechoulam R (1997) Cannabinol derivatives: binding to cannabinoid receptors and inhibition of adenylylcyclase. *J Med Chem* **40**: 3228–3233.

Schlicker E and Kathmann M (2001) Modulation of transmitter release via presynaptic cannabinoid receptors. *Trends Pharmacol Sci* **22**:565-572.

Serre CM, Farlay D, Delmas PD and Chenu C (1999) Evidence for a dense and intimate innervation of the bone tissue, including glutamate-containing fibers. *Bone* **25**:623-629.

Stampa B, Kuhn B, Liess C, Heller M and Gluer CC (2002) Characterization of the integrity of three-dimensional trabecular bone microstructure by connectivity and shape analysis using high-resolution magnetic resonance imaging in vivo. *Top Magn Reson Imaging* **13**:357-363.

Zimmer A, Zimmer AM, Hohmann AG, Herkenham M and Bonner TI (1999) Increased mortality, hypoactivity, and hypoalgesia in cannabinoid CB1 receptor knockout mice. *Proc Natl Acad Sci USA* **96**:5780–5785.

Molecular Pharmacology Fast Forward. Published on June 13, 2006 as DOI: 10.1124/mol.106.026435
This article has not been copyedited and formatted. The final version may differ from this version.

Footnotes

* J.T. and O.O. contributed equally to this article.

Financial support: This work was supported by NIDA grants to RM (9789) and KM (00286, 11322), ISF grants to RM (482/01), and IB and ES (4007/02-Bikura). Purchase of the μCT system was supported in part by ISF grant to IB (9007/01).

Address correspondence to: Prof. Itai Bab, Bone Laboratory, the Hebrew University of Jerusalem, P.O.B. 12272, Jerusalem 91120, Israel. Tel.: 972-2-675-8572; Fax: 972-2-675-7623; Email: babi@cc.huji.ac.il

Molecular Pharmacology Fast Forward. Published on June 13, 2006 as DOI: 10.1124/mol.106.026435
This article has not been copyedited and formatted. The final version may differ from this version.

Legends for Figures

Figure 1. CB1 is expressed in sympathetic nerve fibers in trabecular bone. A-B, RT-PCR analysis in (A) bone marrow stromal cells undergoing osteoblastic differentiation in "osteogenic medium"; note absence of CB1-positive bands. PTHRc1, PTH receptor 1; TNSALP, tissue non-specific alkaline phosphatase. NOM, cells grown for 20 days in non-osteogenic medium (negative control); C, cerebellar mRNA (positive control). (B) bone marrow-derived monocytic cells undergoing osteoclastogenesis in medium containing M-CSF and RANKL; Ocl, osteoclast-like TRAP-positive multinucleated cells. Mon, undifferentiated monocytes. C, cerebellar mRNA (positive control). Cells were derived from WT C57Bl/6J mice. C-H, immunohistochemical staining in secondary spongiosa in distal femoral metaphysis from $C57^{CB1-/-}$ (C-F) and $CD1^{CB1-/-}$ (G-H) mice. (C, D, G) anti tyrosine hydroxylase antibodies; (E, F, H) consecutive sections stained with anti CB1 antibodies. T, bone trabeculae; arrows, osteoblasts; arrow heads, tyrosine hydroxylase-CB1 positive fibers. Hematoxylin counterstaining.

Figure 2. Bone mass phenotype in CB1-null mice. Tri-dimensional µCT images of distal femoral metaphysial trabecular bone from mice with median bone volume density (BV/TV) values. Quantitative data are mean±SEM obtained in 16 $C57^{CB1-/-}$ and 16 WT C57Bl/6J mice per gender, 6 $CD1^{CB1-/-}$ and 6 WT CD1 males and 20 $CD1^{CB1-/-}$ and 20 WT CD1 females. $*P< 0.05$.

Figure 3. µCT-based structural morphometric parameters in secondary spongiosa of distal femoral metaphysis of CB1-null mice. A-C, $C57^{CB1-/-}$ mice and their WT C57Bl/6J controls; D-F, $CD1^{CB1-/-}$ mice and their WT CD1 controls. (A, D) trabecular number. (B, E) trabecular thickness (C, F) trabecular connectivity. Data are mean±SEM obtained in 16 $C57^{CB1-/-}$ and 16 WT C57Bl/6J mice per gender, 6 $CD1^{CB1-/-}$ and 6 WT CD1 males and 20 $CD1^{CB1-/-}$ and 20 WT CD1 females. $*P< 0.05$.

Molecular Pharmacology Fast Forward. Published on June 13, 2006 as DOI: 10.1124/mol.106.026435
This article has not been copyedited and formatted. The final version may differ from this version.

Figure 4. μCT-based measurements of diaphyseal dimensions in CB1-null mice. A-C, $C57^{CB1-/-}$ mice and their WT C57Bl/6J controls; D-F, $CD1^{CB1-/-}$ mice and their WT CD1 controls. (A, D) overall mid-diaphyseal diameter. (B, E) mid-diaphyseal medullary cavity diameter (C, F) cortical thickness. Data are mean±SEM obtained in 16 $C57^{CB1-/-}$ and 16 WT C57Bl/6J mice per gender, 6 $CD1^{CB1-/-}$ and 6 WT CD1 males and 20 $CD1^{CB1-/-}$ and 20 WT CD1 females. *P< 0.05.

Figure 5. Histomorphometric bone remodeling parameters in secondary spongiosa of distal femoral metaphysis of $C57^{CB1-/-}$ mice. (A) bone formation rate. (B) mineral appositional rate. (C) mineralizing perimeter. (D) osteoclast number. Data are mean±SEM obtained in 8 mice per condition. *P< 0.05.

Molecular Pharmacology Fast Forward. Published on June 13, 2006 as DOI: 10.1124/mol.106.026435
This article has not been copyedited and formatted. The final version may differ from this version.

Table 1. Trabecular histomorphometric bone remodeling parameters of male CD1$^{CB1-/-}$ mice

Genotype	MAR (μm/day)	Min.Peri (%)	BFR ($mm^3/mm^2/day$)	N.Oc/BS (mm^{-1})
KO	2.82±0.19	54.5±5.91	1.55±0.22	2.71±0.31
WT†	2.73±0.14	46.7±2.53	1.27±0.04	2.49±0.49

MAR, mineral appositional rate; Min.Peri, mineralizing perimeter; BFR, bone formation rate; N.Oc/BS, osteoclasts number. Data are mean±SE in 6 male. †CD1 mice.

Figure 1

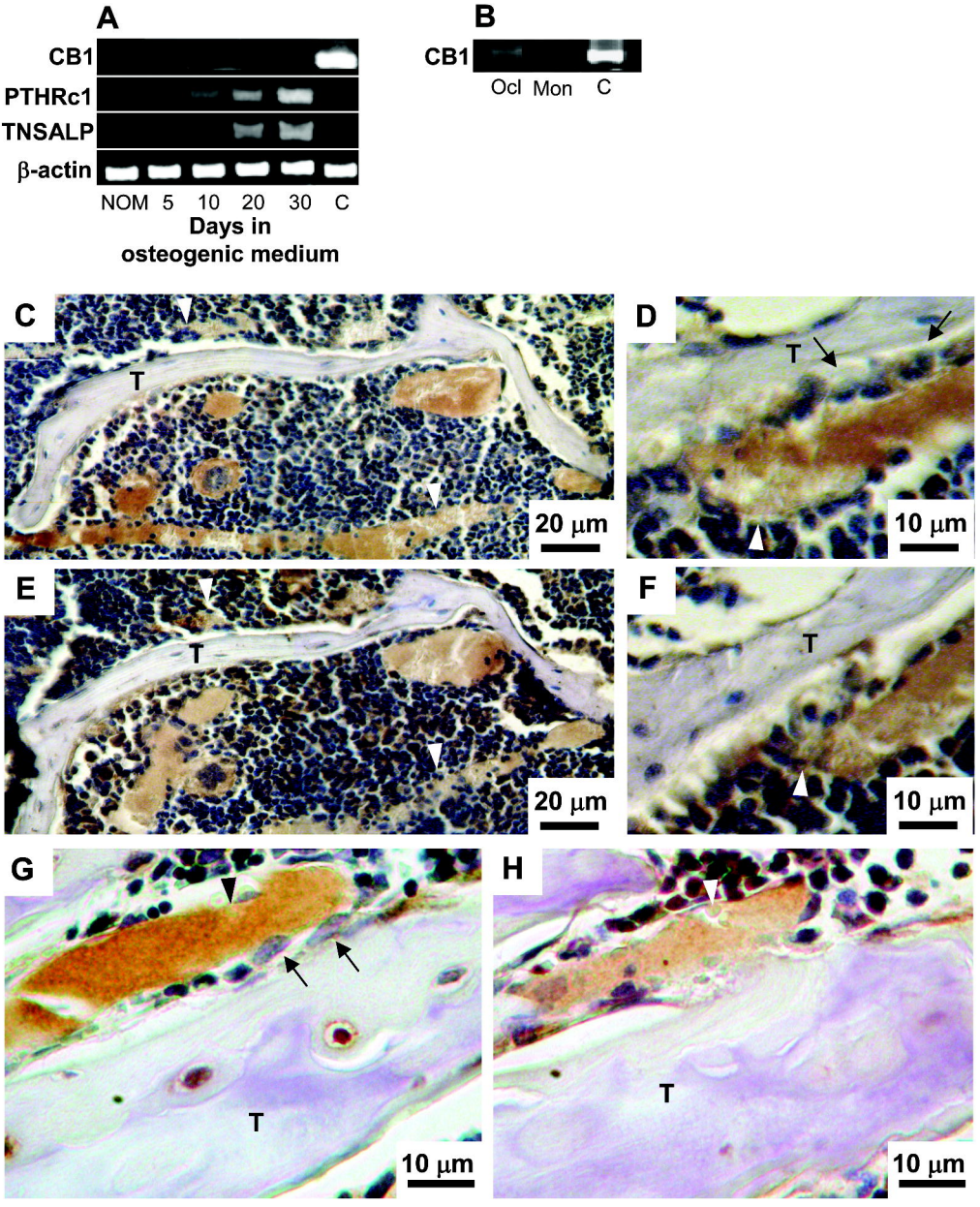
A
CB1
PTHRc1
TNSALP
β-actin
NOM 5 10 20 30 C
Days in osteogenic medium
B
CB1
Ocl Mon C
C
T
20 μm
D
T
10 μm
E
T
20 μm
F
T
10 μm
G
T
10 μm
H
T
10 μm

Figure 2

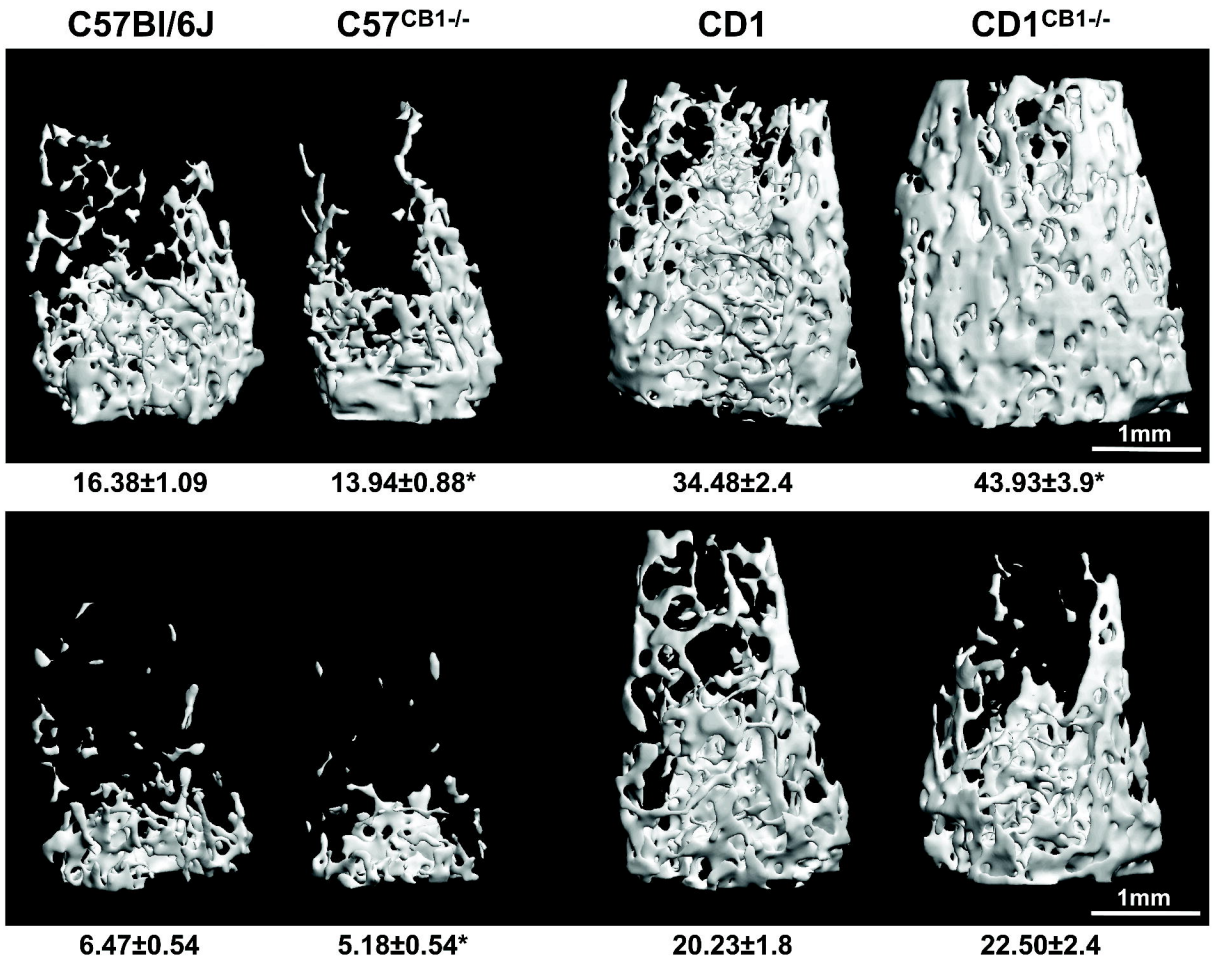
C57Bl/6J
C57CB1-/-
CD1
CD1CB1-/-
Male
1mm
BV/TV (%)
16.38±1.09
13.94±0.88*
34.48±2.4
43.93±3.9*
Female
1mm
BV/TV (%)
6.47±0.54
5.18±0.54*
20.23±1.8
22.50±2.4

Figure 3

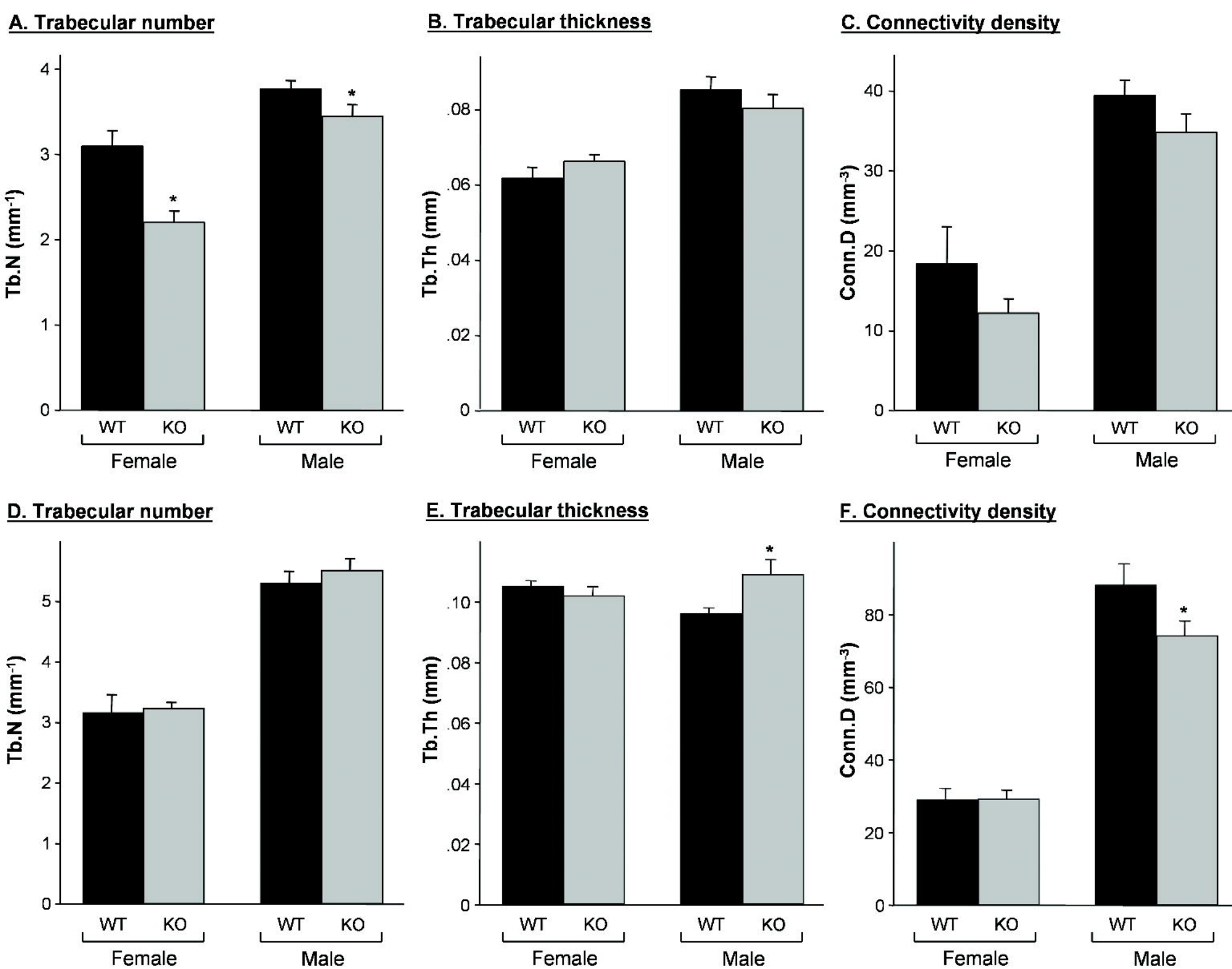
A. Trabecular number
Tb.N (mm-1)
0
1
2
3
4
*
*
WT
KO
WT
KO
Female
Male
B. Trabecular thickness
Tb.Th (mm)
0
.02
.04
.06
.08
WT
KO
WT
KO
Female
Male
C. Connectivity density
Conn.D (mm-3)
0
10
20
30
40
WT
KO
WT
KO
Female
Male
D. Trabecular number
Tb.N (mm-1)
0
1
2
3
4
5
WT
KO
WT
KO
Female
Male
E. Trabecular thickness
Tb.Th (mm)
0
.02
.04
.06
.08
.10
*
WT
KO
WT
KO
Female
Male
F. Connectivity density
Conn.D (mm-3)
0
20
40
60
80
*
WT
KO
WT
KO
Female
Male

Figure 4

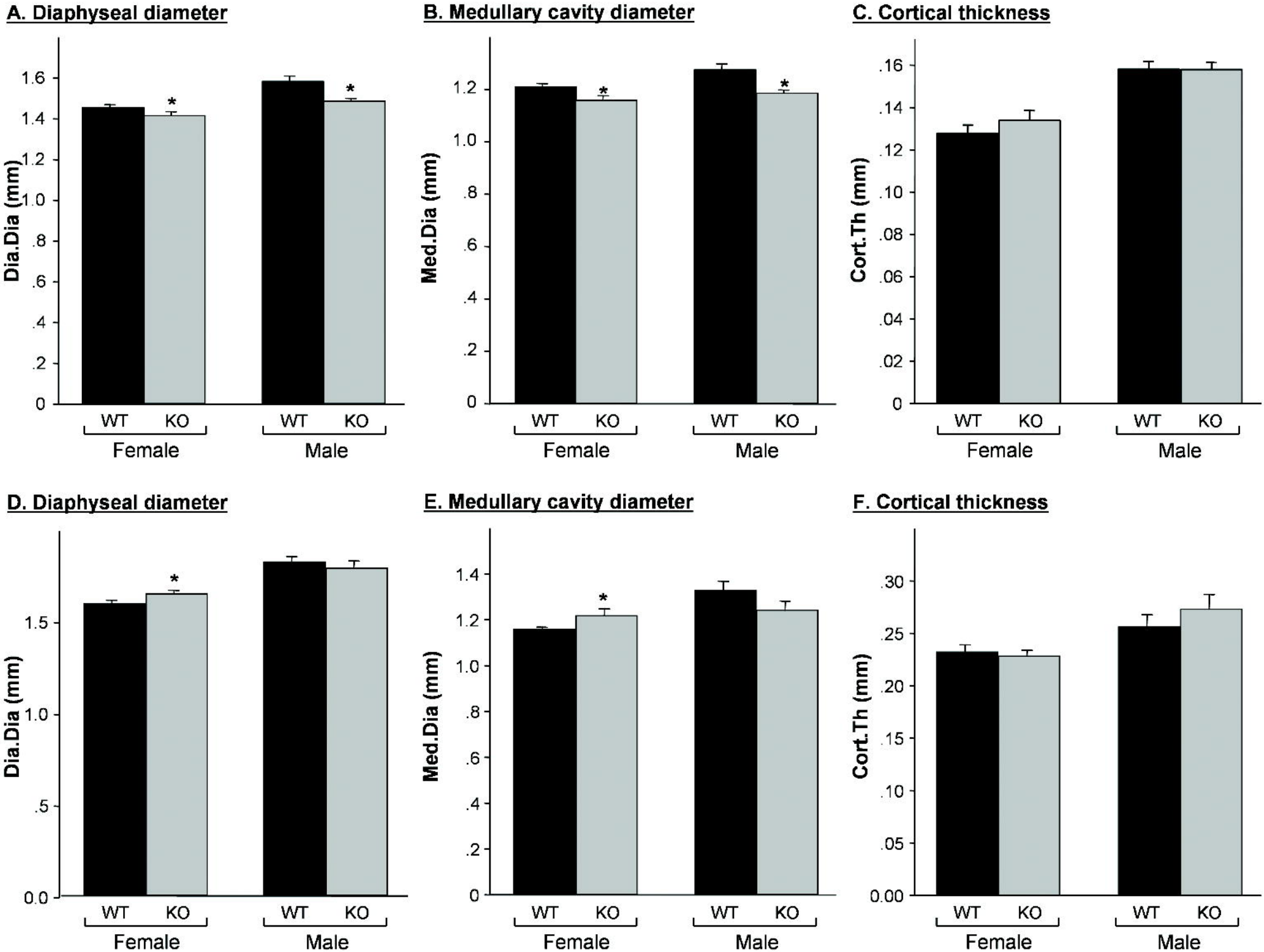
A. Diaphyseal diameter
Dia.Dia (mm)
0
.2
.4
.6
.8
1.0
1.2
1.4
1.6
*
*
WT
KO
WT
KO
Female
Male
B. Medullary cavity diameter
Med.Dia (mm)
0
.2
.4
.6
.8
1.0
1.2
*
*
WT
KO
WT
KO
Female
Male
C. Cortical thickness
Cort.Th (mm)
0
.02
.04
.06
.08
.10
.12
.14
.16
WT
KO
WT
KO
Female
Male
D. Diaphyseal diameter
Dia.Dia (mm)
0.0
.5
1.0
1.5
*
WT
KO
WT
KO
Female
Male
E. Medullary cavity diameter
Med.Dia (mm)
0
.2
.4
.6
.8
1.0
1.2
1.4
*
WT
KO
WT
KO
Female
Male
F. Cortical thickness
Cort.Th (mm)
0.00
.05
.10
.15
.20
.25
.30
WT
KO
WT
KO
Female
Male

Figure 5

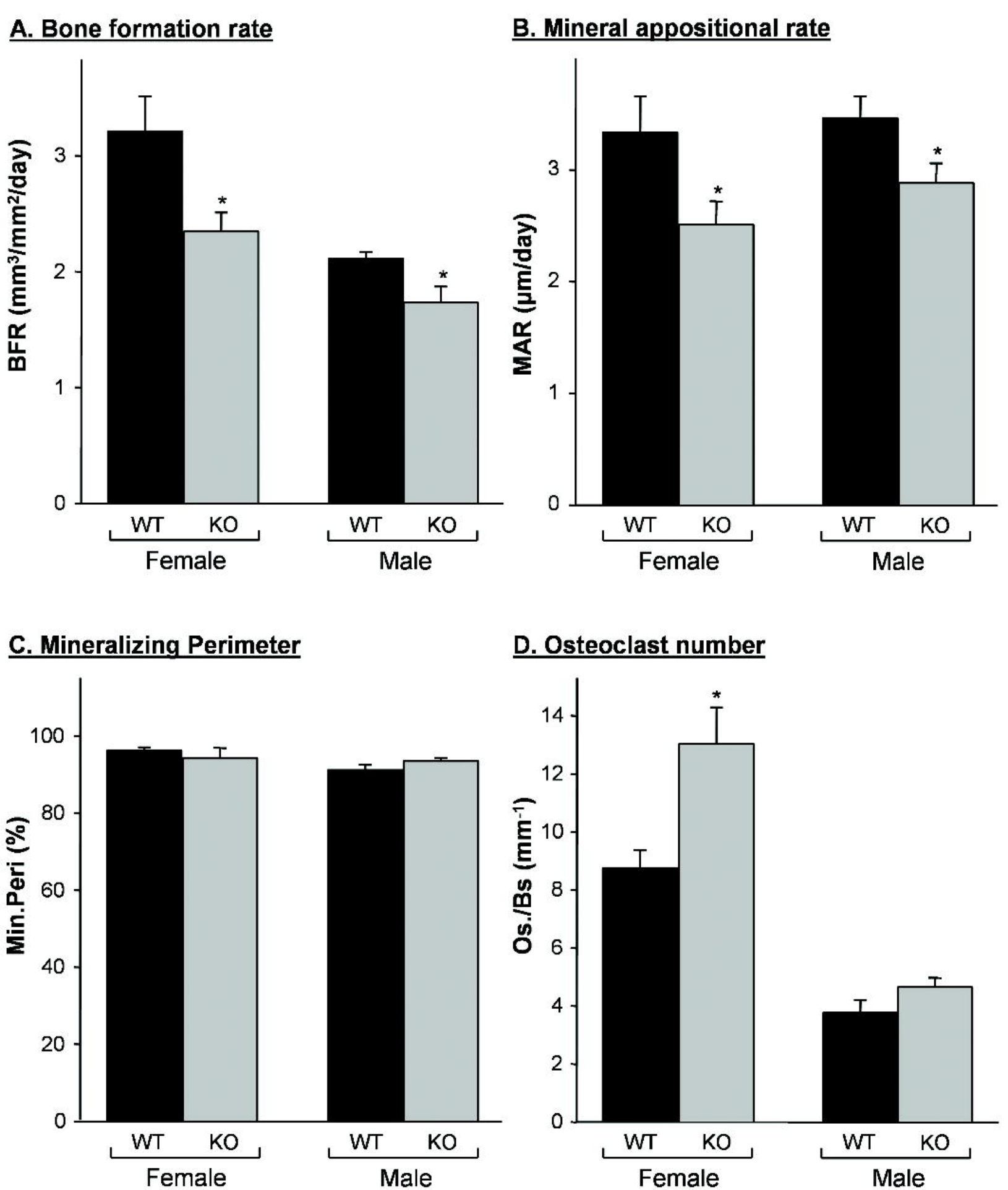
A. Bone formation rate
BFR (mm³/mm²/day)
0
1
2
3
*
*
WT
KO
WT
KO
Female
Male
B. Mineral appositional rate
MAR (µm/day)
0
1
2
3
*
*
WT
KO
WT
KO
Female
Male
C. Mineralizing Perimeter
Min.Peri (%)
0
20
40
60
80
100
WT
KO
WT
KO
Female
Male
D. Osteoclast number
Os./Bs (mm⁻¹)
0
2
4
6
8
10
12
14
*
WT
KO
WT
KO
Female
Male